2010.10.20 Liang Yin

Efficient Synthesis Triggered by Site-Selective Oxidations of Aliphatic C-H Bonds

1. Introduction

Scheme 1 Representative Total Syntheses of Taxol.

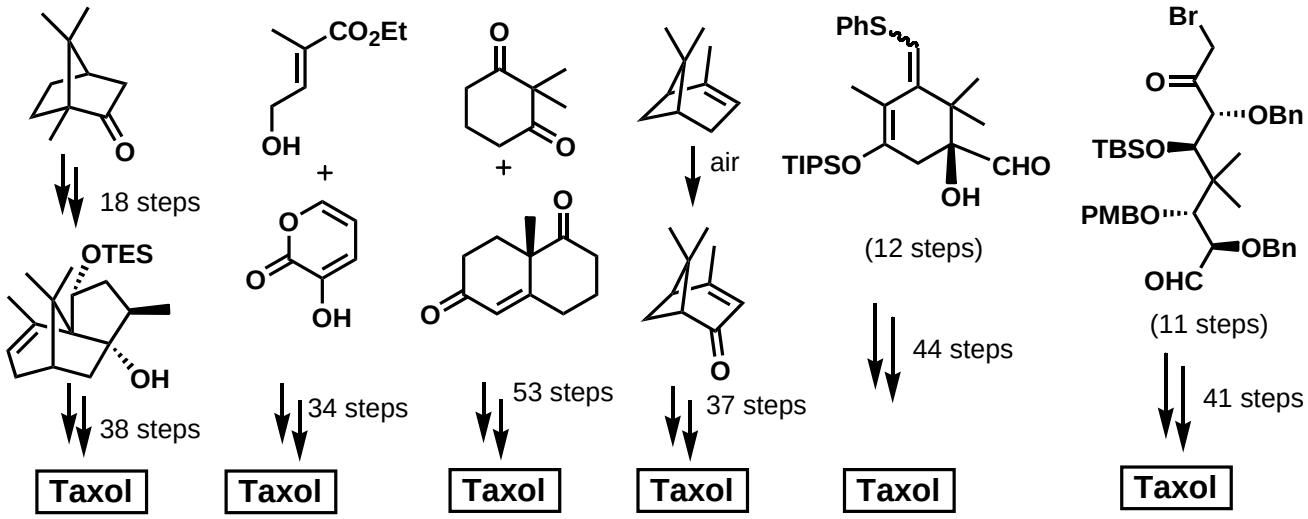

Holton *JACS* **1994,** ***116*****, 1597;** *JACS* **1994,** ***116*****, 1599.**

Nicolaou *Nature* **1994,** ***367*****, 630.**

Danishefsky *JACS* **1996,** ***118*****, 2843.**

Wender *JACS* **1997,** ***119*****, 2755;** *JACS* **1997,** ***119*****, 5757.**

Kuwajima *JACS* **1998,** ***120*****, 12980;** *JACS* **2000,** ***122*****, 3811.**

Mukaiyama *Chem. Eu. J.* **1999,** ***5*****, 121.**

Scheme 2 Biosynthesis of Taxanes (solid arrows imply demonstrated steps).

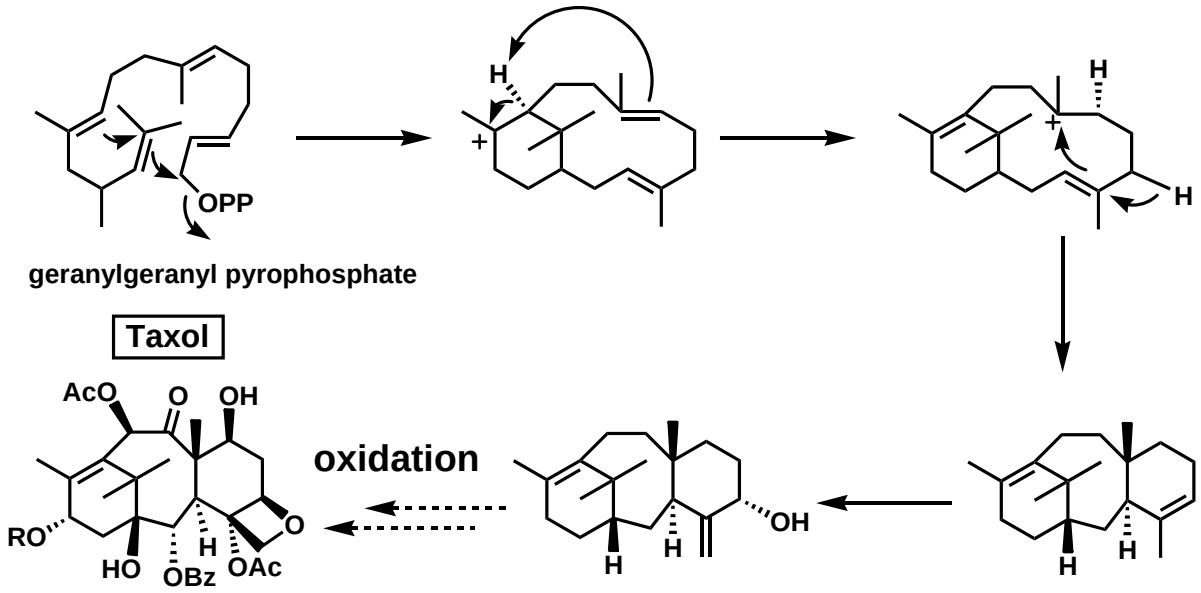

biological interest:

impressive anticancer activity;

unprecedented mode of action.

synthetic interest:

intriguing 6-8-6 tricyclic skeleton;

***anti*-Bredt olefin**

highly oxidized framework

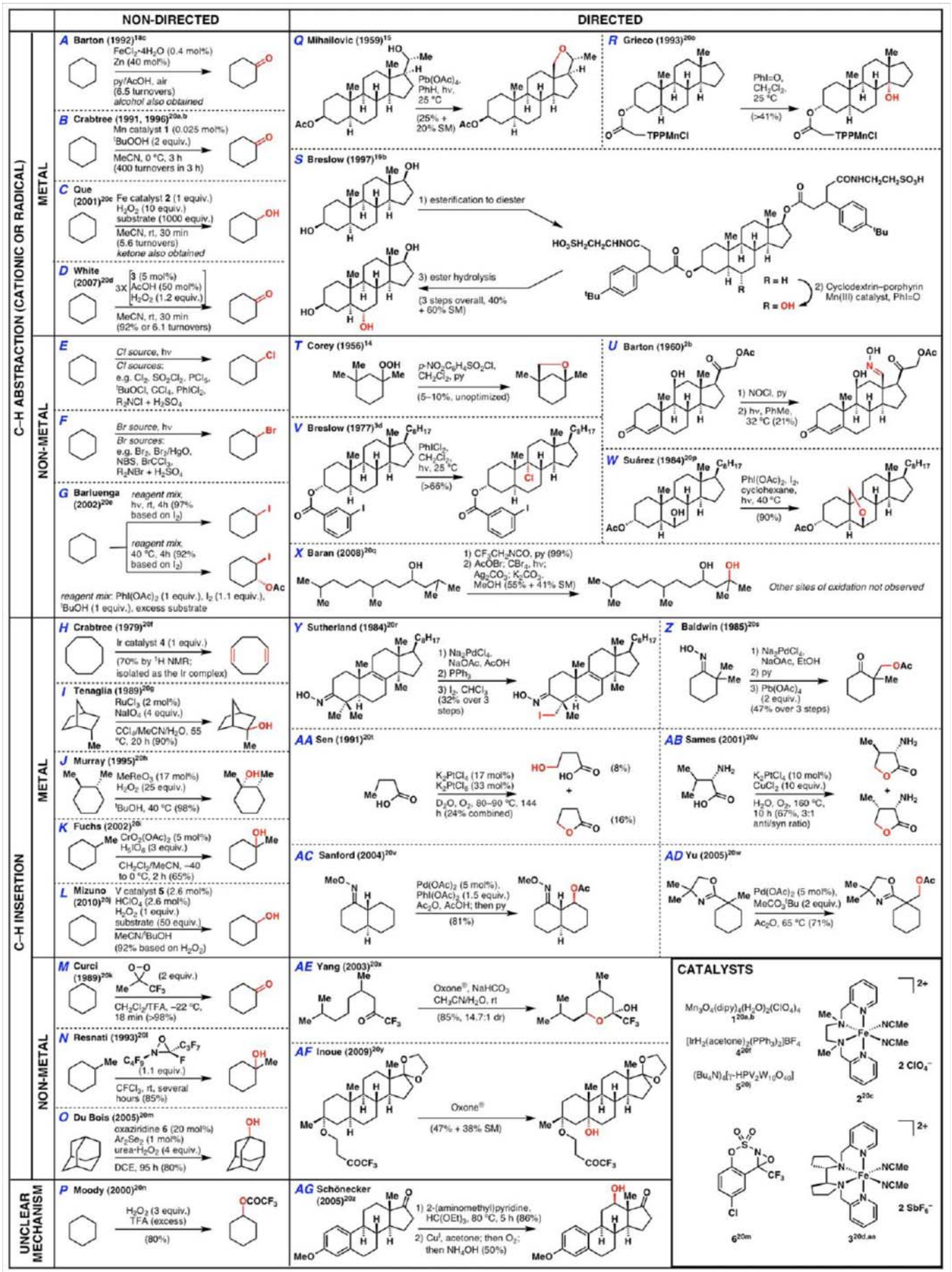

Scheme 1 Examples of non-directed and directed C_{sp3}–H functionalization methods to generate halides and oxygen-containing functionality; oxidations engendered by the given reaction are indicated in red.

2. Developments in Site-Selective Oxidations of Aliphatic C-H Bond Since 2000

2.1 Oxidations of Aliphatic C-H without Catalytic Amount of Metals

Yang Dan *J. Org. Chem.* **2003**, *68*, 6321.

TABLE 1. Selective Oxidation of δ C−H Bond[a]

entry	ketone	Product (Yield %)[b]
1	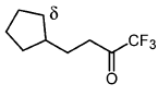 **3**	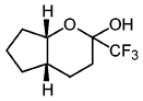 **3a** (74%)
2	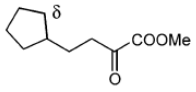 **4**	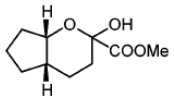 **4a** (67%)
3[c]	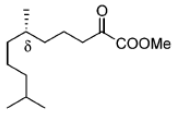 **5**	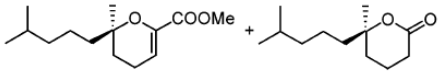 **5a** (78%)[d] **5b** (8%)
4	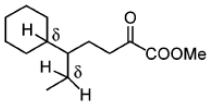 **6**	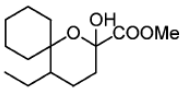 **6a** (73%)[e]

[a] Unless otherwise indicated, all reactions were carried out with a 10 mM solution of ketone in a 1.5:1 mixture of CH_3CN and aqueous Na_2·EDTA solution (0.4 mM) containing 5.0 equiv of Oxone and 15.0 equiv of $NaHCO_3$ for 24 h at room temperature. [b] Isolated yield after flash column chromatography. [c] Reaction was carried out for 6 h, and the reaction temperature was increased from 0 °C to room temperature after the addition of the mixture of Oxone and $NaHCO_3$. [d] 73% ee; determined by HPLC. [e] **6a** was obtained as a 4:1 mixture of diastereomers.

Yang Dan *JACS* **1998**, *120*, 6611.

SCHEME 1. Selective Oxidation of δ C−H Bond

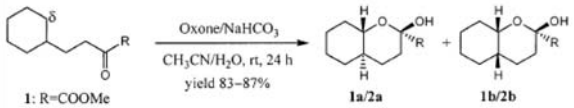

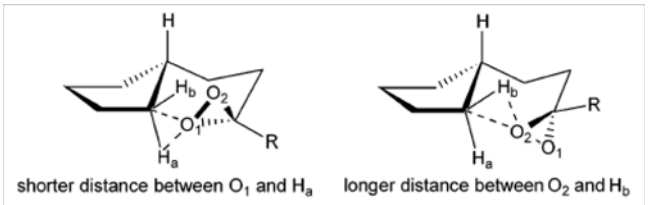

FIGURE 3. Possible transition state for the oxidation reactions of ketones **3** and **4**.

SCHEME 4. Possible Pathway for the Formation of Lactone 5b

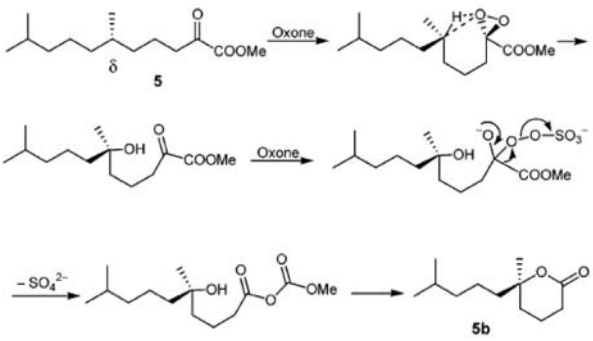

Scheme 5

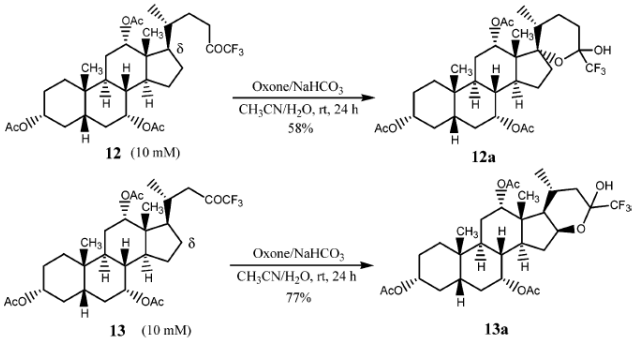

M. Inoue *Org. Lett.* **2009**, *11*, 3630.

Table 1. Construction of 1,3-Diaxial Diol Derivatives from Various Carbocycles[a]

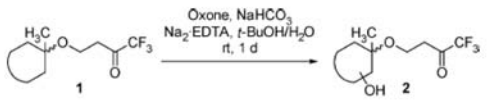

entry	starting material (sm)	product	yield, % product (sm)	yield, % brsm[b]
1	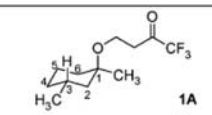 1A	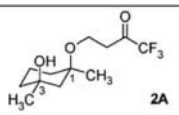 2A	51 (31)	74
2[c]	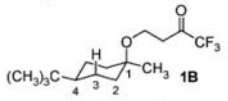 1B	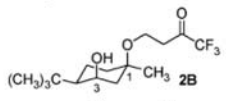 2B	14 (43)	25
3	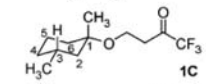 1C	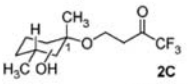 2C	0 (64)	0
4	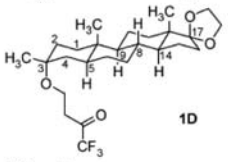 1D	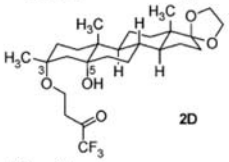 2D	47 (38)	76
5	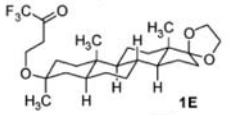 1E	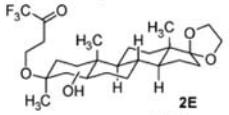 2E	0 (63)	0
6[c]	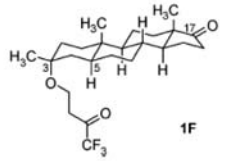 1F	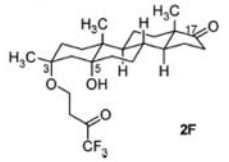 2F	33 (16)	39

[a] The starting material was treated with Oxone (5 equiv) and $NaHCO_3$ (15 equiv) in *t*-BuOH/0.4 mM aq Na_2·EDTA solution = 3/2 (0.01 M) at rt for 1 d. [b] Yield based on the recovered starting material. [c] MeCN/0.4 mM aq Na_2·EDTA solution = 3/2 (0.0015 M) was used as a solvent.

2.2 Oxidations of Aliphatic C-H Bonds Catalyzed by Metals

Sanford *JACS* **2004**, *126*, 9542.

Table 1. Selectivity of Unactivated sp^3 C–H Bond Oxidation[a]

Entry	Substrate	Major Product	Yield[b]
1	 (4)	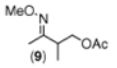 (9)	74%[c]
2	 (5)	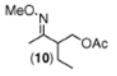 (10)	78%[c]
3	 (6)	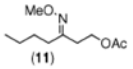 (11)	39%[c]
4	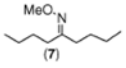 (7)	No Reaction	0%
5	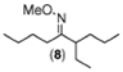 (8)	No Reaction	0%

[a] 1 equiv of substrate (0.12 M), 1.1 equiv of $PhI(OAc)_2$, 5 mol % $Pd(OAc)_2$, 50% AcOH/50% Ac_2O, 100 °C, 1.5–3.5 h. [b] Isolated yields. [c] Isolated as a mixture of oxime *E*/*Z* isomers.

Table 2. Substrate Scope of sp^3 C–H Bond Oxygenation[a]

Entry	Substrate	Product	Yield[b]
1	 (12)	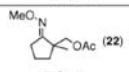 (22)	61%
2	 (13)	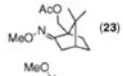 (23)	75%
3	 (14)	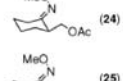 (24)	81%[c]
4	(15)	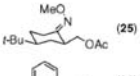 (25)	86%[c]
5	 (16)	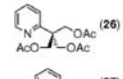 (26)	63%
6	 (17)	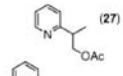 (27)	42%
7	 (18)	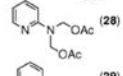 (28)	70%
8	 (19)	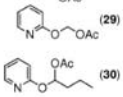 (29)	66%
9	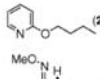 (20)	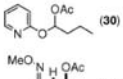 (30)	44%
10	 (21)	(31)	81%

[a] 1 equiv of substrate (0.12 M), 1.1–3.2 equiv of $PhI(OAc)_2$, 5 mol % $Pd(OAc)_2$, in AcOH, 50% AcOH/50% Ac_2O, or CH_2Cl_2, 80–100 °C, 5 min–12 h. [b] Isolated yields. [c] Isolated as a mixture of oxime E/Z isomers.

Sanford *OL* **2010**, *12*, 532.

Yu Jin-Quan *Angew. Chem. Int. Ed.* **2005**, *44*, 7420.

Table 1. *O*-Acetyl Oxime-Directed Acetoxylation of C−H Bonds[a]

entry	starting material	product	yield[b]
1[c]	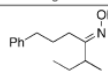	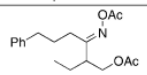	49% (70%)[d]
2[c]		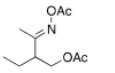	61%
3[c]	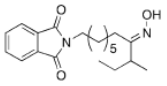	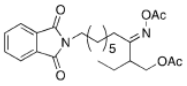	65%
4[c]	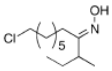	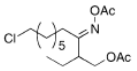	33%
5[c]		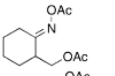	66%
6			41%

[a] Conditions: 0.12 M in AcOH/Ac_2O (1:1), 2 h, 25 °C; then 5 mol % $Pd(OAc)_2$, 1−3 equiv of $PhI(OAc)_2$, 80 or 100 °C, 4−12 h. [b] The remaining mass balance (as determined by GC of the crude reaction mixtures) was generally unreacted *O*-acetyloxime (analogous to **8** in eq 3). [c] Starting material and product consisted of a mixture of oxime *E*/*Z* stereoisomers.

Table 1: $Pd(OAc)_2$-catalyzed oxidation of methyl groups by MeCOOO*t*Bu.[a]

Entry	Substrate	Product	Yield [%]
1	 **1**	 **1d**	71
2	 **2**	 **2a**	62
3	 **3**	 **3a**	69
4	 **4**	 **4a** 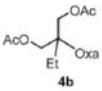 **4b**	89
5	 **5**	 **5a**	90
6	 **6**	 **6a**	68
7	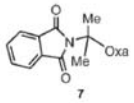 **7**	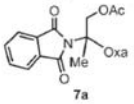 **7a**	50
8	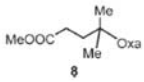 **8**	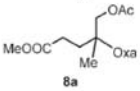 **8a**	70
9	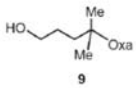 **9**	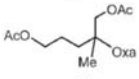 **9a**	50

[a] Oxa = 2-substituted 4,4-dimethyloxazoline. Reaction conditions: entries 1–5, $Pd(OAc)_2$ (5 mol%), Ac_2O, MeCOOO*t*Bu (2 equiv), 65 °C, 48–72 h; entries 6–9, $Pd(OAc)_2$ (10 mol%). In the absence of air or pure O_2, the reaction stopped at 30–40% conversion and the precipitation of P

Table 2: $Pd(OAc)_2$-catalyzed diastereoselective oxidation of methyl groups by lauroyl peroxides.[a]

Entry	Substrate	Product	Yield [%]	*de* [%]
1	 **10**	 **10a**	67	18
2	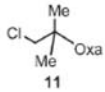 **11**	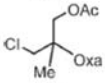 **11a**	66	38
3	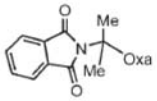 **12**	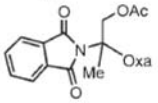 **12a**	38	12
4	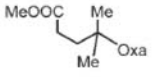 **13**	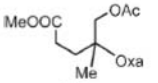 **13a**	73	24
5	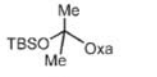 **14**	**14a**	43	62
6	**15**	**15a**	49	82

[a] Oxa = 2-substituted 4-*tert*-butyloxazoline. Reaction conditions: $Pd(OAc)_2$ (5 mol%), Ac_2O, lauroyl peroxide (2 equiv), 50 °C, 48 h. The presence of air or pure O_2 increases the conversion rate.

Figure 2. X-ray crystal structure of **16a**.

Scheme 3. Formation of chiral trinuclear $C(sp^3)$–Pd complex **16a**.

Bruno Schonecker *Tetrahedron* **2005**, *61*, 103.

Scheme 1 β-Hydroxylation of the Nonactivated C-H Bonds.

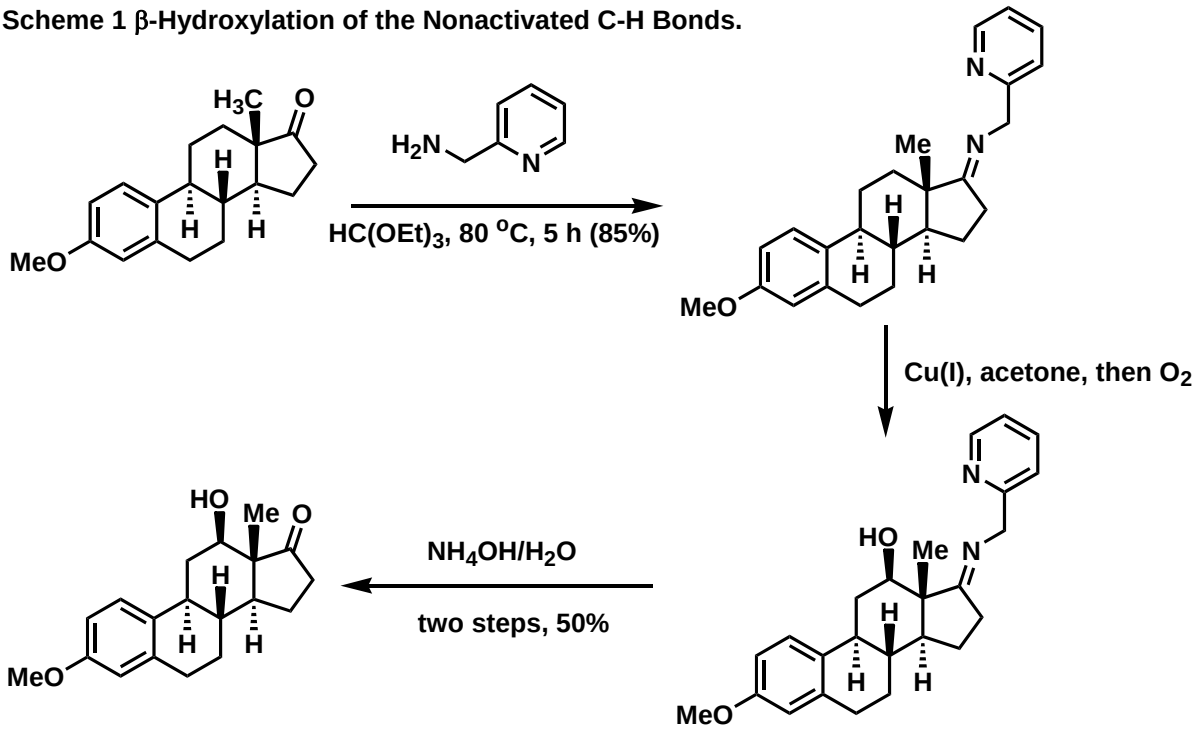

Scheme 2. Proposed Mechanism for β-Hydroxylation.

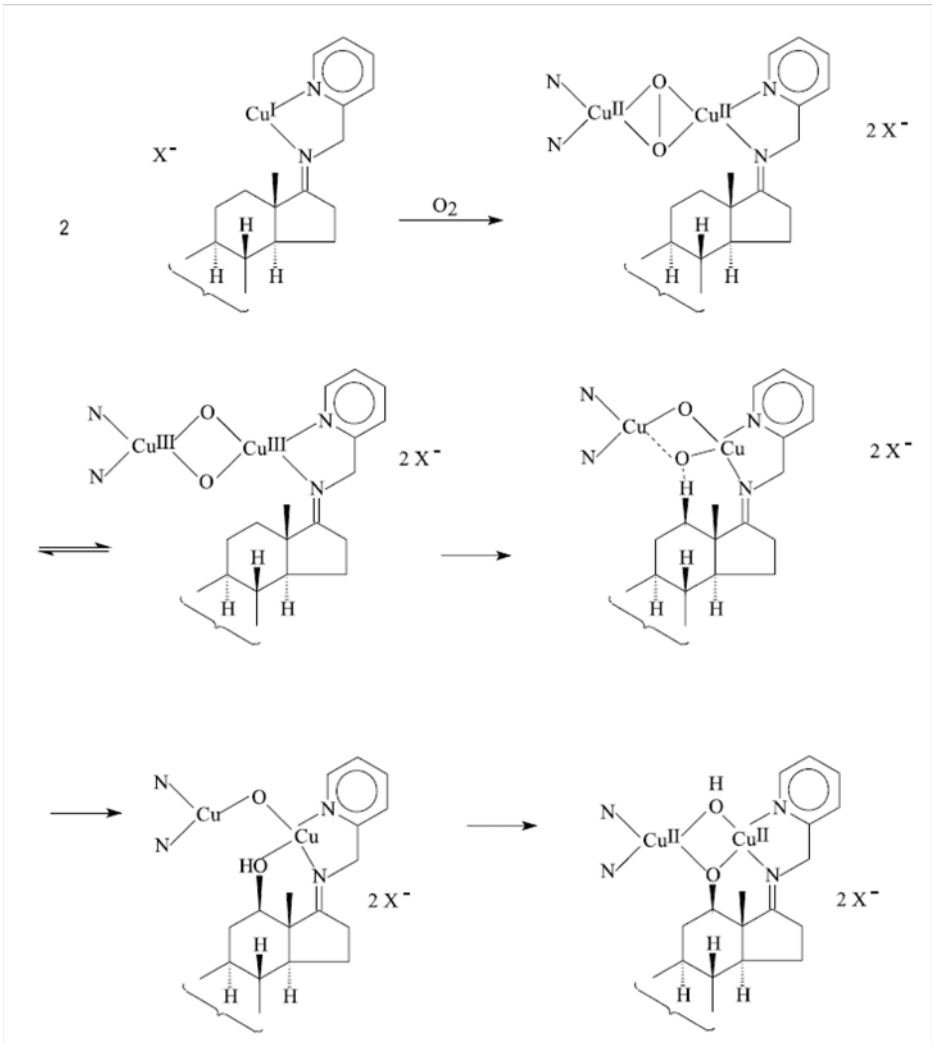

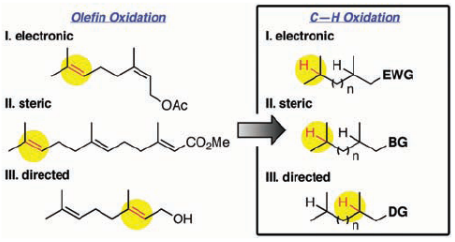

Fig. 1. Comparison between established modes of site-selective olefin oxidations and proposed modes for site-selective C–H bond oxidations with bulky, electrophilic metal catalysts. BG indicates bulky group; DG, directing group. (I) In asymmetric dihydroxylations (AD) catalyzed by electrophilic OsO_4 with bulky quinuclidine ligands, dihydroxylation of polyenes occurs preferentially at the most electron-rich double bond (highlighted in yellow). (II) In AD, the most sterically accessible olefin site (yellow) is dihydroxylated preferentially. (III) Olefinic alcohols are epoxidized site-selectively with $Mo(CO)_6$, $VO(acac)_2$, or $Ti(DET)(O\text{-}i\text{-}Pr)_2$. acac, acetylacetonate; DET, diethyl tartrate.

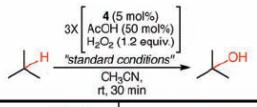

Entry	Product	Isolated % Yield (rsm)*	Entry	Product	Isolated % Yield (rsm)*
1	**5**, X = Br	46 (26)	6	(+)-**10**, Z = H	57 (27)
2	**6**, X = OAc	53 (43)	7	(+)-**11**, Z = OAc	43 (42)
3	**7**	60 (18)	8	(-)-**12**	33 (67) 90† (6)
4	**8**	43 (33)	9	**13**	52 (20)
5	**9**	52 (21)	10	**14**	92‡

*rsm = % recovered unoxidized starting material. †Starting material was recycled five times. ‡GC yield.

Fig. 3. Evaluation of functional group compatibility and substrate scope in **4**-catalyzed oxidations of unactivated sp^3 C–H bonds with H_2O_2. "Standard conditions" entail dropwise addition of a solution of H_2O_2 over ca. 45 to 75 s at room temperature [(50 weight % (wt %), 1.2 equivalents (equiv.) in CH_3CN at 0.13 M] to a solution of **4** [5 mole % (mol %)], AcOH (0.5 equiv.), and substrate in CH_3CN (0.67 M). After 10 min, a second portion of **4** (5 mol%) and AcOH (0.5 equiv.) in CH_3CN (0.05 M) is added, followed by dropwise addition of H_2O_2 (50 wt %, 1.2 equiv.) in CH_3CN (0.13 M); a third addition is then done in the same manner for a total of 15 mol % **4**, 1.5 equiv. AcOH, and 3.6 equiv. of H_2O_2. Products resulting from unselective and overoxidation were observed in trace amounts by ^{1}H-NMR analysis of the crude reaction mixture.

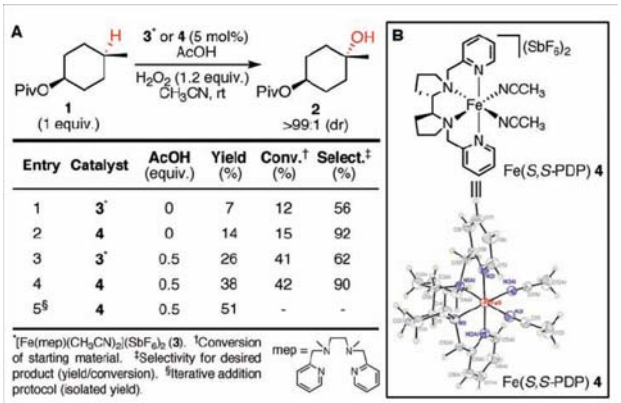

Entry	Catalyst	AcOH (equiv.)	Yield (%)	Conv.† (%)	Select.‡ (%)
1	**3***	0	7	12	56
2	**4**	0	14	15	92
3	**3***	0.5	26	41	62
4	**4**	0.5	38	42	90
5§	**4**	0.5	51	-	-

*[Fe(mep)(CH3CN)2](SbF6)2 (**3**). †Conversion of starting material. ‡Selectivity for desired product (yield/conversion). §Iterative addition protocol (isolated yield).

Fig. 2. (**A**) Development of a preparatively useful aliphatic C–H oxidation reaction. Products resulting from unselective and overoxidation were observed in trace amounts by ^{1}H nuclear magnetic resonance (NMR) and gas chromatograph analysis of the crude reaction mixture. (**B**) Structure of $[Fe(S,S\text{-}PDP)(CH_3CN)_2](SbF_6)_2$ catalyst (**4**) based on x-ray crystallographic analysis (anions are omitted for clarity). PDP indicates 2-({(*S*)-2-[(*S*)-1-(pyridin-2-ylmethyl)pyrrolidin-2-yl]pyrrolidin-1-yl}methyl)pyridine.

Fig. 4. (**A**) Reactivity trends for oxidations catalyzed by **4** based on the electronics of the C–H bond. (**B**) Substrate electronic effects on site selectivity in hydroxylations of multiple 3° C–H bonds with **4**. Only small amounts of diol byproducts were observed. (**C**) DFT-calculated three-dimensional structure of the lowest potential energy conformer of (–)-**23** with corresponding calculated electrostatic atomic charges (eV) of the 3° C–H bonds of interest. (**D**) Selective hydroxylation of (–)-**23** at C-1 with **4** based on steric effects. For standard conditions see, Fig. 3. Aliphatic C–H bonds that are oxidized to form product are indicated in red.

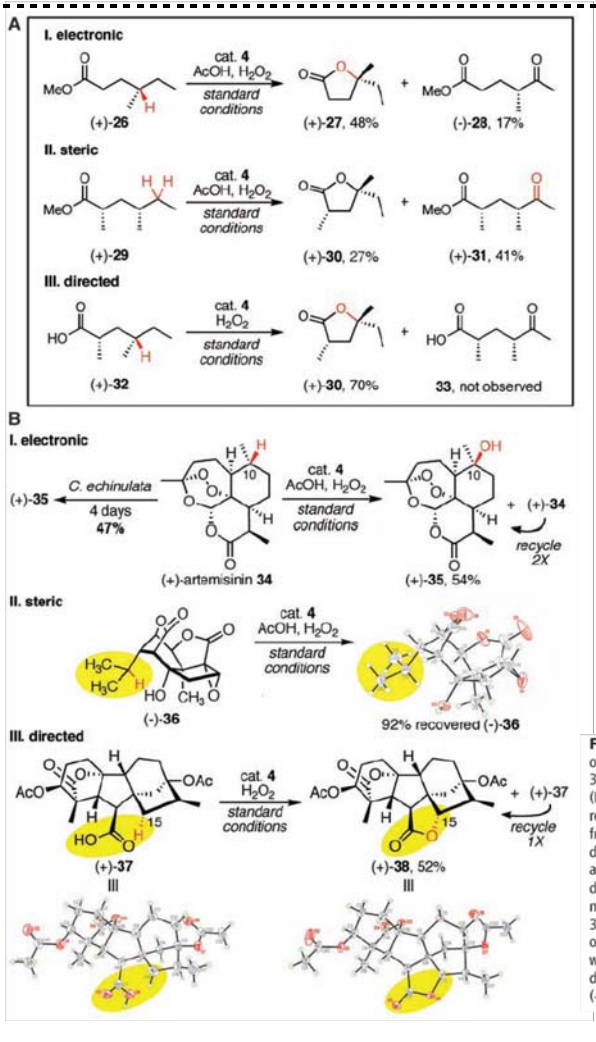

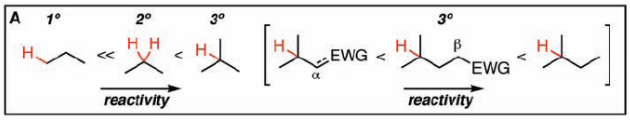

B

Entry	Substrate	Major Product	Isolated %Yield* (rsm)†	[Remote: Proximal]‡
1	remote proximal	**15**, X = H	48§(29)	1:1
2		**16**, X = OAc	43 (35)	5:1
3		**17**, X = Br	39 (32)	9:1
4		**18**, X = F	43 (20)	6:1
5		**19**, X = OAc	49 (21)	29:1
6		**20**, X = Br	48 (17)	20:1
7		**21**, R = CH_3	52 (18)	>99:1
8		**22**, R = OCH_3	56 (32)	>99:1

*Unless otherwise noted, isolated yields are of pure major product isolated from the entire reaction mixture. †rsm = % recovered unoxidized starting material. ‡GC analysis of crude reaction mixture using authentic standards. §Isolated as a 1:1 mixture of remote:proximal.

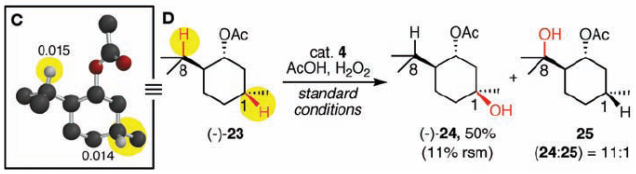

Fig. 5. (**A**) Three modes of selective aliphatic C–H bond oxidation catalyzed by **4**. Aliphatic C–H bonds that are oxidized to form major product are indicated in red. (I) Oxidation occurs preferentially at the most electron-rich 3° C–H bond followed by in situ lactonization. Unoxidized (+)-**26** was recovered in 23% yield from the reaction. (II) Oxidation occurs at the least sterically hindered, most electron-rich methylene site. Unoxidized (+)-**29** was recovered in 16% yield from the reaction. (III) Oxidation is directed to the sterically hindered 3° C–H site by the free carboxylic acid. (**B**) Predictably selective aliphatic C–H bond oxidations with **4** of natural products and their derivatives. (I) Selective oxidation of **34** with small molecule catalyst **4** and with cultures of *C. echinulata* occurs at the most electron-rich and least sterically hindered 3°C–H bond to furnish (+)-**35**. (II) Structure of (-)-**36**, determined by x-ray analysis. When (–)-**36** was exposed to standard reaction conditions, 92% of the starting material was recovered because of electronic deactivation of the core and steric deactivation of the isopropyl 3° C–H bond. (III) Carboxylate-directed lactonization of tetrahydrogibberellic acid analog (+)-**37** via C-H oxidation to form lactone (+)-**38** in 52% isolated yield (recycled once). The structures of (+)-**37** and (+)-**38** were determined by x-ray crystallographic analysis and are shown below. For substrates with carboxylic acid directing groups [i.e., (+)-**32** and (+)-**37**], AcOH additive was omitted. For acid-sensitive substrates [i.e., (+)-**34**], AcOH additive was lowered to 10 mol % per addition.

2.3 Application of Oxidations of Aliphatic C-H Bonds in the Total Synthesis of Eudesmane Terpenes

P. S. Baran *Nature* **2009**, *459*, 824.

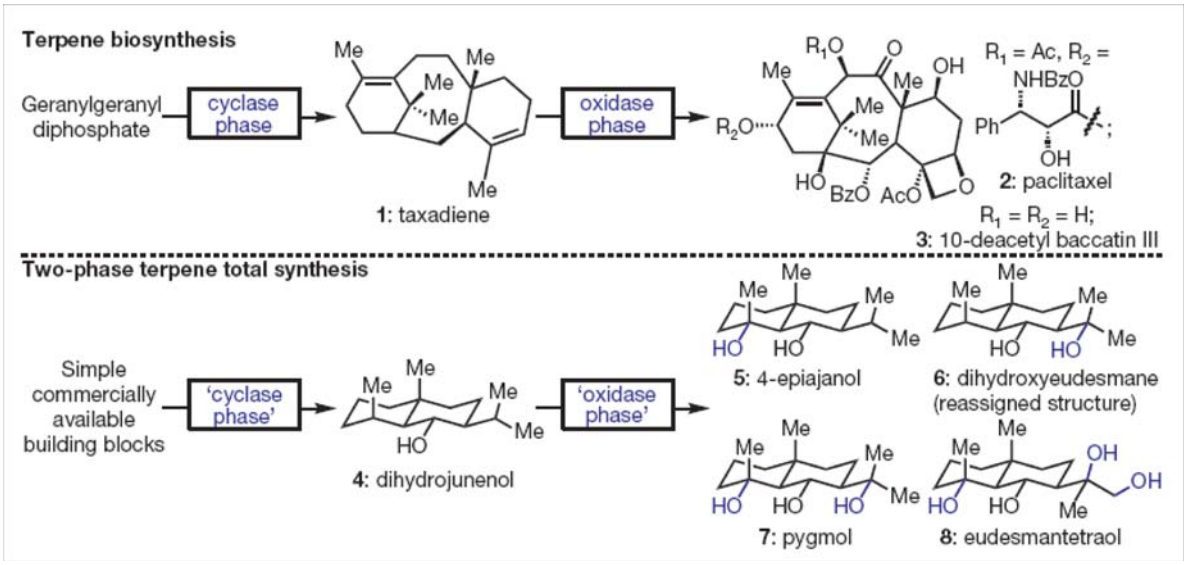

Figure 1 | Outline of the 'two-phase' approach to terpene total synthesis. Me, methyl; Ac, acetyl; Bz, benzoyl.

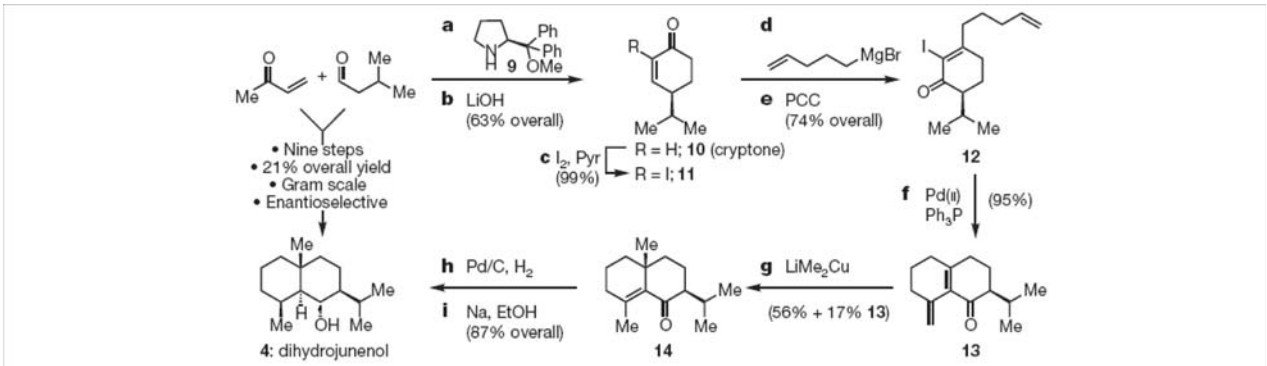

Figure 2 | Simple, enantioselective total synthesis of dihydrojunenol (4). Reagents and conditions as follows. **a**, Methyl vinyl ketone (1.5 equiv.), 3-methyl butyraldehyde (1.0 equiv.), prolinol catalyst (0.05 equiv.), ethyl 3,4-dihydroxybenzoate (0.20 equiv.), neat, 4 °C, 36 h, 89%. **b**, LiOH (0.1 equiv.), *i*-PrOH, room temperature (RT, 23 °C), 24 h, 63% over two steps, 89% enantiomeric excess. **c**, I_2 (1.2 equiv.), Pyr/DCM, RT, 12 h, 99%. **d**, $(CH_2CHCH_2CH_2CH_2)MgBr$ (1.5 equiv.), toluene, −78 °C, 30 min; then 0 °C, 30 min. **e**, PCC (1.2 equiv.), 3 Å MS, DCM, RT, 6 h, 74% over two steps. **f**, $Pd(OAc)_2$ (0.1 equiv.), Ph_3P (0.3 equiv.), Et_3N (1.2 equiv.), Ag_2CO_3 (1.0 equiv.), CH_3CN, 70 °C, 3 h, 95%. **g**, $LiMe_2Cu$ (1.5 equiv.), DCM, 0 °C, 4 h, 56% (17% recovered starting material). **h**, H_2 (1 atm), Pd/C (0.1 equiv.), EtOAc, RT, 30 min. **i**, Na (5 equiv.), EtOH, RT, 30 min, 87% over two steps. Et_3N, triethylamine; DCM, dichloromethane; I_2, iodine; Pyr, pyridine; PCC, pyridinium chlorochromate; MS, molecular sieves; Ph_3P, triphenylphosphine; CH_3CN, acetonitrile; $LiMe_2Cu$, lithium dimethylcuprate; EtOAc, ethyl acetate. For selected physical data for compounds **11**, **12**, **13**, **14** and **4**, see the Supplementary Information.

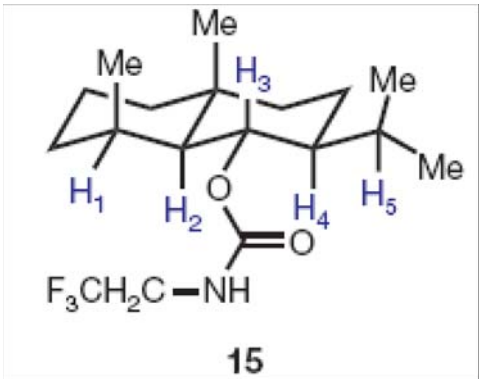

$$\delta_{C3} = 73.6 \text{ p.p.m.} > \delta_{C2} = 55.2 \text{ p.p.m.} \approx \delta_{C4} = 50.2 \text{ p.p.m.} > \delta_{C1} = 27.5 \text{ p.p.m.} \approx \delta_{C5} = 26.6 \text{ p.p.m.}$$

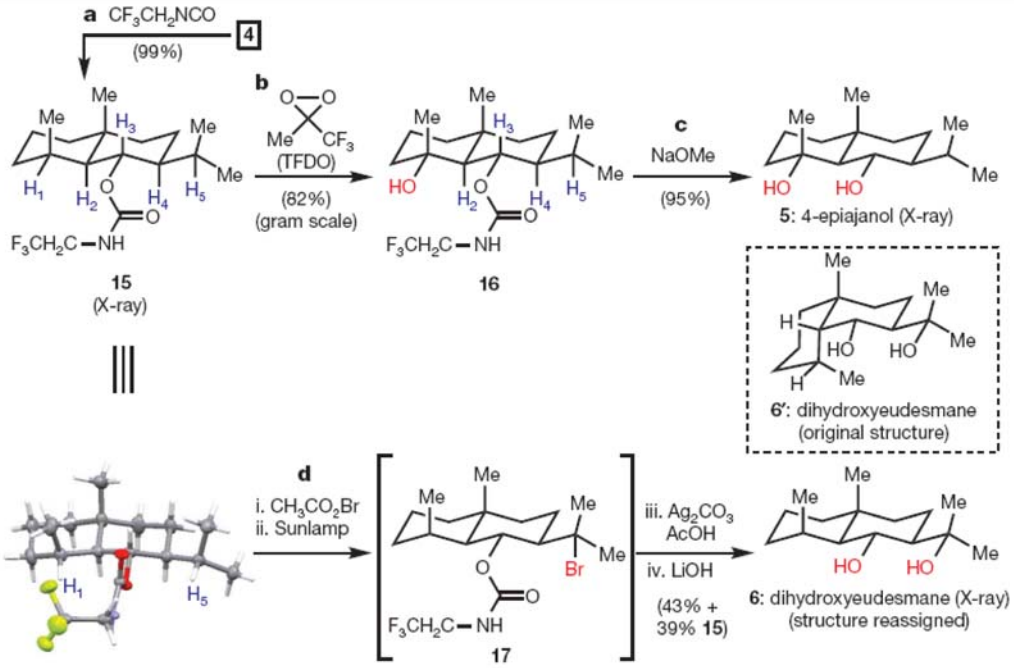

Figure 3 | Total syntheses of 4-epiajanol (5) and dihydroxyeudesmane (6) through site-specific C–H oxidations of dihydrojunenol (4). Reagents and conditions as follows. **a**, CF_3CH_2NCO (1.0 equiv.), Pyr (4.0 equiv.), DMAP (catalytic), DCM, RT, 1 h, 99%. **b**, TFDO (1.0 equiv.), DCM, −20 °C, portion-wise addition of TFDO over 30 min, then additional 30 min, 82%. **c**, NaOMe (5.0 equiv.), MeOH, 70 °C, 2 h, 95%. **d**, CH_3CO_2Br (1.0 equiv.), DCM, 0 °C, 5 min; $PhCF_3$, 100-W sunlamp, 10 min; Ag_2CO_3 (1.2 equiv.), DCM, RT, 30 min, then aqueous acetic acid, RT, 30 min; LiOH (10 equiv.) THF/H_2O, RT, 10 min, 43% (39% recovered **15**). DMAP, 4-dimethylaminopyridine; TFDO, methyl(trifluoromethyl)dioxirane; NaOMe, sodium methoxide; THF, tetrahydrofuran. For selected physical data for compounds **5**, **6**, **15** and **16**, see the Supplementary Information. Compounds **5**, **6** and **15** were verified by X-ray crystallography.

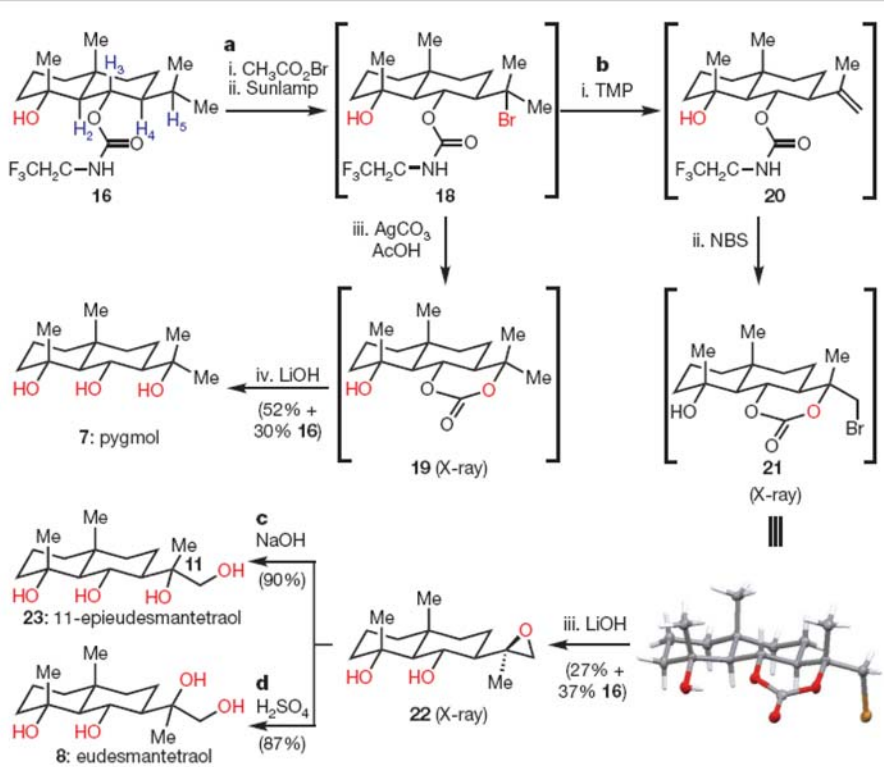

Figure 4 | Total syntheses of pygmol (7) and eudesmantetraol (8) through site-specific C–H oxidations of 16. Reagents and conditions as follows. **a**, CH_3CO_2Br (1.0 equiv.), DCM, 0 °C, 5 min; $PhCF_3$, 100-W sunlamp, 20 min; Ag_2CO_3 (1.2 equiv.), DCM, RT, 30 min, then aqueous acetic acid, RT, 30 min; LiOH (10 equiv.), THF/H_2O, RT, 10 min, 52% (30% recovered **16**). **b**, TMP (2.0 equiv.), toluene, 80 °C, 12 h; NBS (2.0 equiv.), DCM, RT, 6 h, then aqueous acetic acid, RT, 30 min; LiOH (10 equiv.), THF/H_2O, RT, 10 min, 27% (37% recovered **16**). **c**, 3 M NaOH, DMSO, 80 °C, 2 h, 90%. **d**, 0.1 M H_2SO_4, DME/H_2O, RT, 1 h, 87%. TMP, 2,2,6,6-tetramethylpiperidine; NBS, *N*-bromosuccinimide; DMSO, dimethylsulphoxide; DME, 1,2-dimethoxyethane. For selected physical data for compounds **7**, **8**, **19**, **21**, **22** and **23**, see the Supplementary Information. Compounds **19**, **21** and **22** were verified by X-ray crystallography.

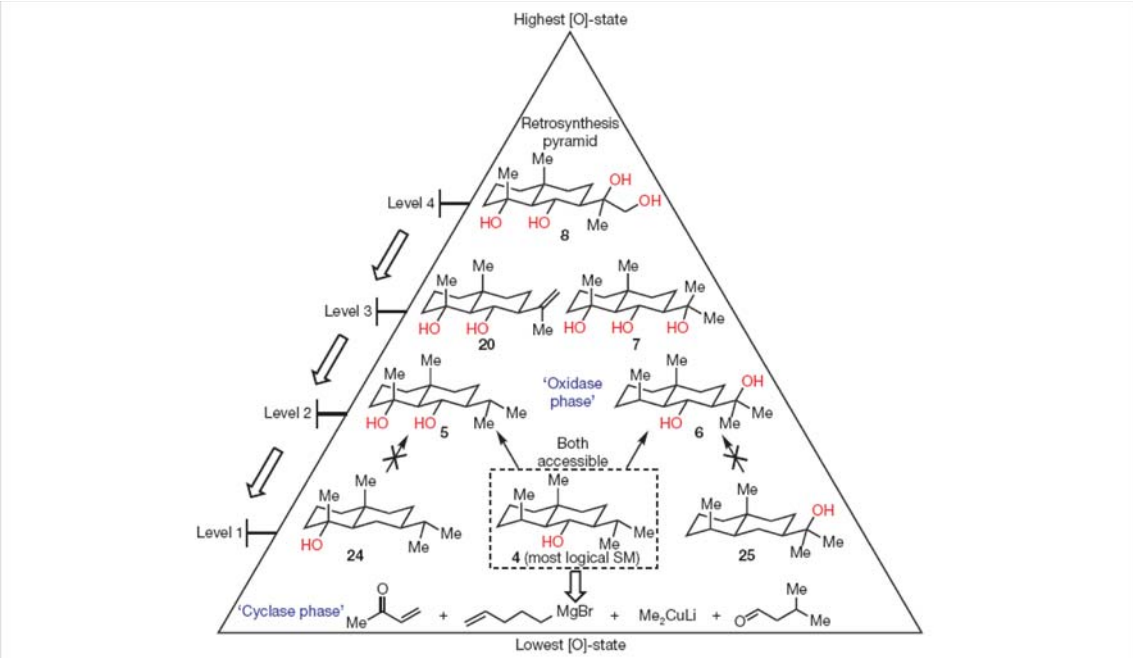

Figure 5 | Pyramid diagram for the retrosynthetic planning of terpene synthesis using a 'two-phase' approach. Because eudesmantetraol (**8**) is the highest oxidized target, it is placed at the apex. Removal of one hydroxyl group leads to level-3 intermediates **20** and **7** (and any synthetic equivalents such as an alkyl bromide, for example **18** in Fig. 4). Repetition of this transform leads to diols **5** and **6** (level 2), either of which could conceivably access **20** or **7**. Subsequent deoxygenation of these level-2 intermediates leads to three selections for level 1: **24**, **4** and **25**. Dihydrojunenol (**4**) was chosen as the most logical starting material owing to its potential to access both **5** and **6** without any corrective reduction steps or a difficult C–H activation of a methylene group. [O]-state, oxidation state; SM, starting material.

2.4 Application of Oxidations of Aliphatic C-H Bonds in the Total Synthesis of Taxol (on the way)

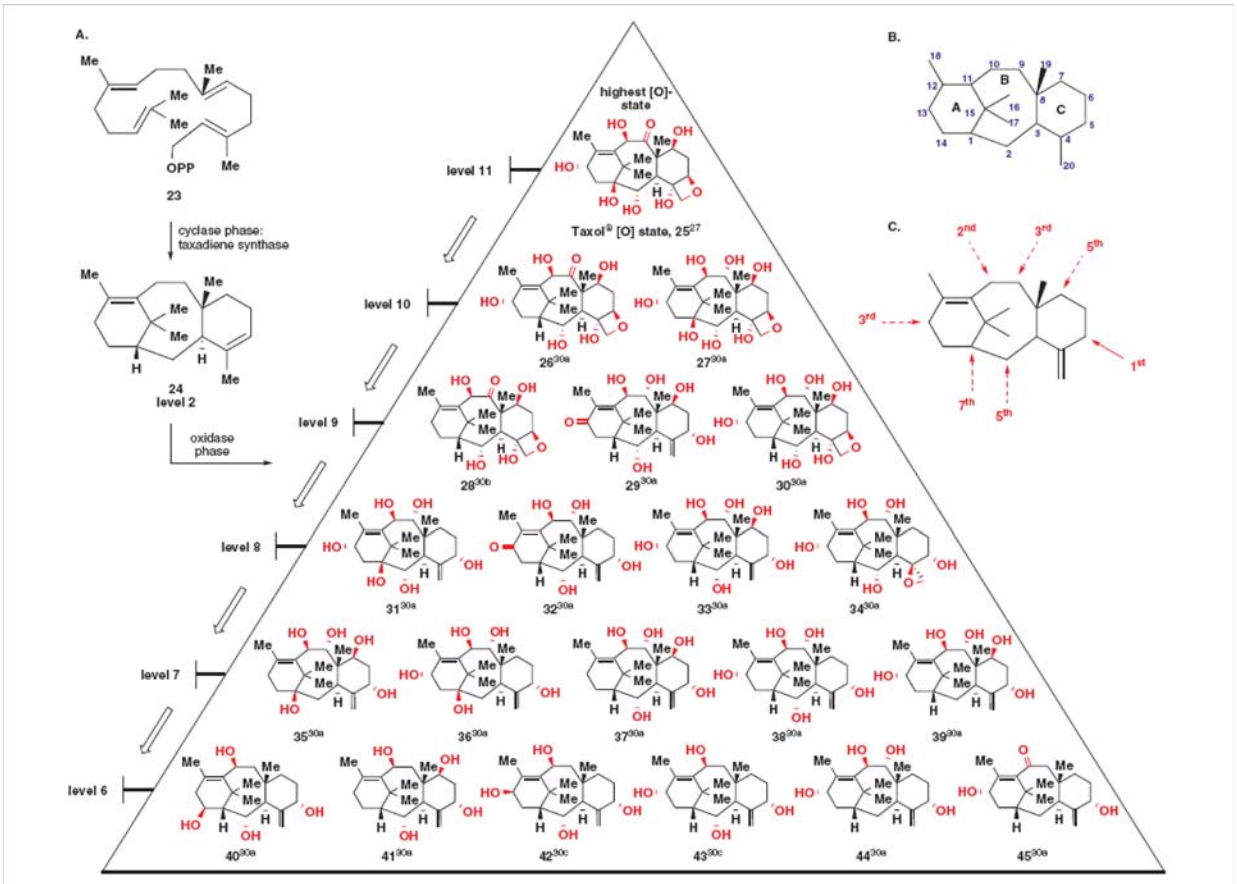

Figure 2 A) Taxane biosynthesis and 'oxidase phase pyramid' for the retrosynthetic planning of taxane synthesis using a two-phase approach; B) taxane carbon and ring numbering; C) assumed oxygenation sequence of taxadiene in Nature.[33] Notes: 1) This is not a comprehensive list of all taxane oxidation patterns; 2) for clarity and discussion purposes, all side chains attached to hydroxyl groups were omitted; 3) all taxanes in the above pyramid are found in Nature, and these natural products are indicated with isolation paper references; 4) any additional oxidations installed onto taxadiene **24** are indicated in red.

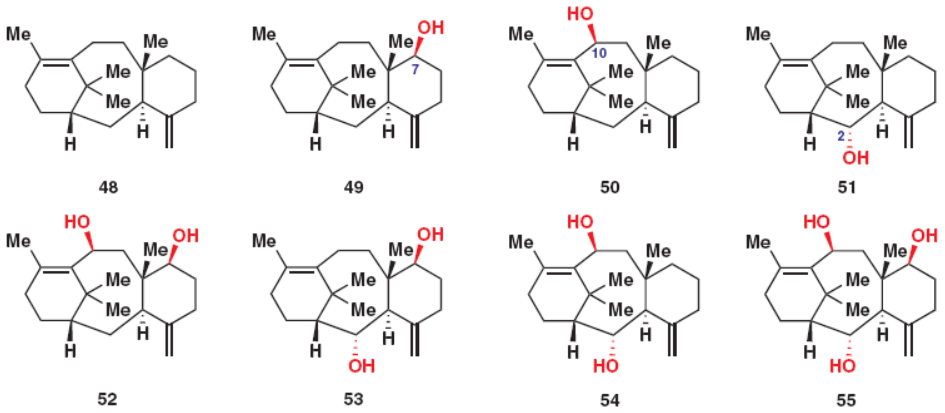

Figure 4 Potential cyclase phase endpoints for the two-phase synthesis of taxanes; any additional oxidations installed onto taxadiene **48** are indicated in red.

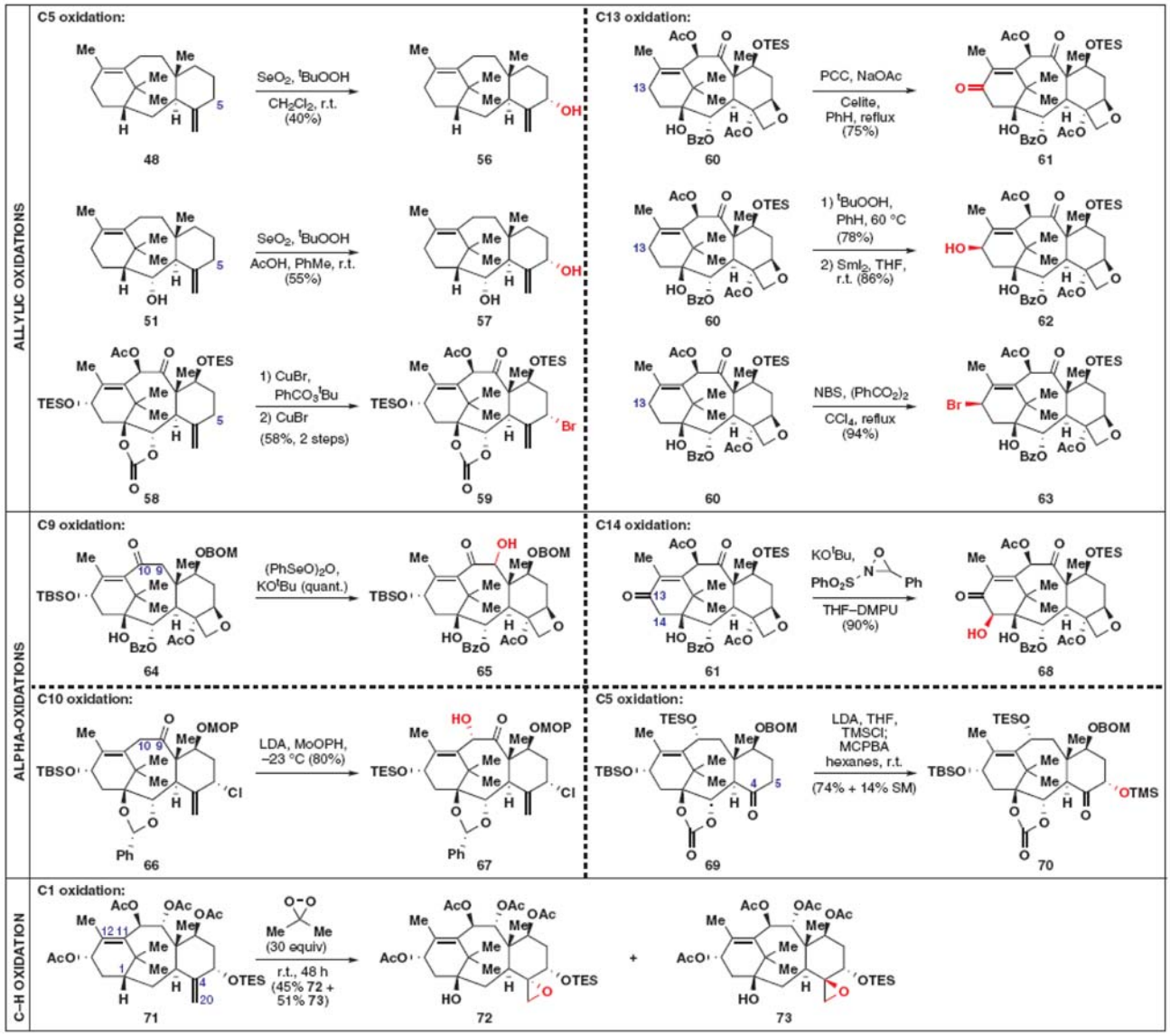

Scheme 4 Known oxidative transformations in taxanes; oxidations engendered by the given reaction are indicated in red.

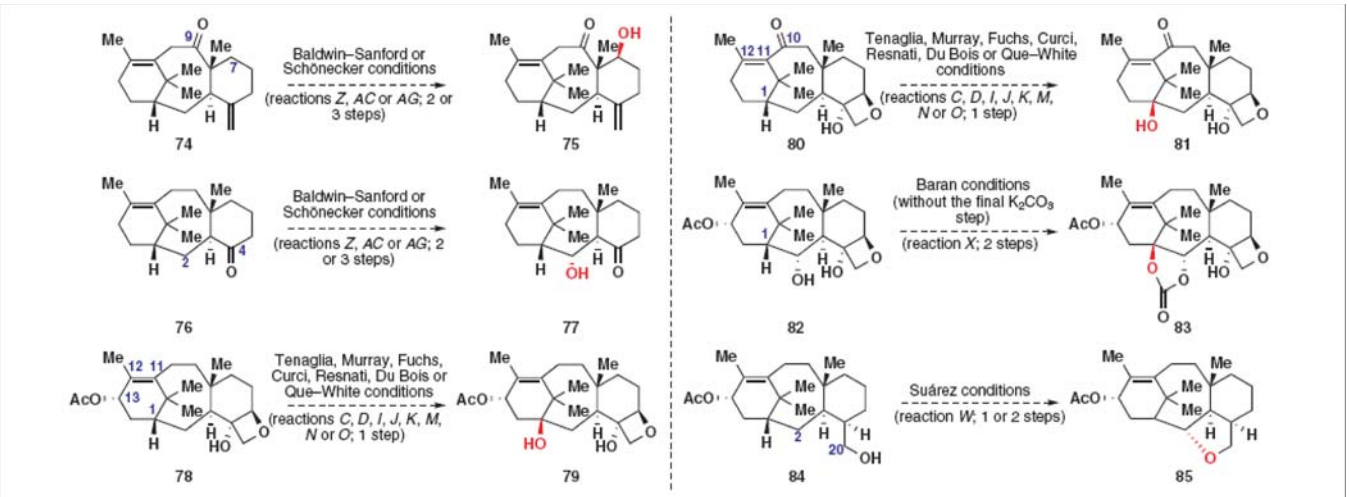

Scheme 5 Potential applications of C–H oxidation in the taxane framework; please see Scheme 1 for reaction labeling; projected oxidations engendered by the given reaction are indicated in red.

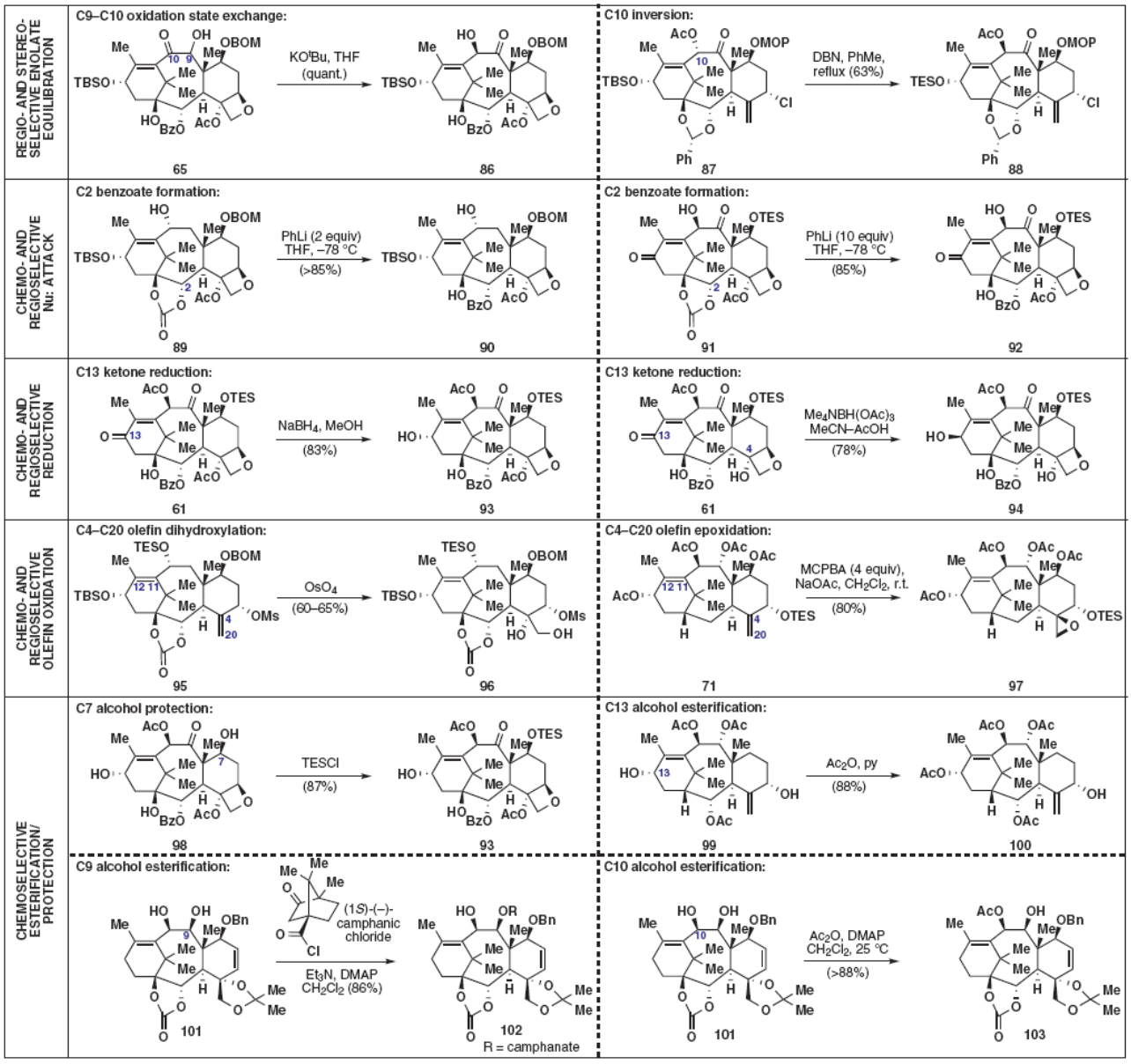

Scheme 6 Chemo-, regio-, and/or stereoselective transformations in taxanes.

3. Conclusions and Outlook

Some of the opportunities for innovation include:

1) The development of a practical and versatile means of achieving controllable dehydrogenation (a synthetic desaturase);

2) new methods to override inherent C-H bond reactivity without recourse to directing groups; design and synthesis of new efficient metal complex like White's iron catalyst 4 would be of primary importance;

3) new multipurpose directing groups, which in some cases cases might be more useful than a reagent-only approach;

4) strategic innovation in the design and execution of a highly practical (gram-scale), minimally oxidized hydrocarbon synthesis (cyclase phase);

5) Extention of current oxidation of aliphatic C-H bonds t to construction of C-N bonds and C-C bonds to greatly increasing the synthetic efficiency.